

1 Quantifying the effects of  
2 non-pharmaceutical and pharmaceutical  
3 interventions against COVID-19 epidemic in  
4 the Republic of Korea: Mathematical  
5 model-based approach considering age  
6 groups and the Delta variant

7 Youngsuk Ko<sup>1</sup>, Victoria May P. Mendoza<sup>1</sup>, Yubin Seo<sup>2</sup>, Jacob  
8 Lee<sup>2</sup>, Yeonju Kim<sup>3</sup>, Donghyok Kwon<sup>3</sup>, and Eunok Jung<sup>1,\*</sup>

9 <sup>1</sup>Department of Mathematics, Konkuk University

10 <sup>2</sup>Division of Infectious Disease, Department of Internal  
11 Medicine, Kangnam Sacred Heart Hospital, Hallym University  
12 College of Medicine

13 <sup>3</sup>Division of Public Health Emergency Response Research, Korea  
14 Disease Control and Prevention Agency

15 \*Corresponding author

16 \*\*Word count: 3186

17

## Abstract

18

### Background:

19

20

21

22

23

24

### Methods:

25

26

27

28

29

30

31

32

33

### Results:

34

35

36

37

38

39

40

41

42

43

### Conclusions:

44

45

46

Early vaccination efforts and non-pharmaceutical interventions were insufficient to prevent a surge of coronavirus disease 2019 (COVID-19) cases triggered by the Delta variant. This study aims to understand how vaccination and variants contribute to the spread of COVID-19 so that appropriate measures are implemented.

A compartment model that includes age, vaccination, and infection with the Delta or non-Delta variants was developed. We estimated the transmission rates using maximum likelihood estimation and phase-dependent reduction effect of non-pharmaceutical interventions (NPIs) according to government policies from 26 February to 8 October 2021. We extended our model simulation until 31 December considering the initiation of eased NPIs. Furthermore, we also performed simulations to examine the effect of NPIs, arrival timing of Delta variant, and speed of vaccine administration.

The estimated transmission rate matrices show distinct pattern, with the transmission rates of younger age groups (0-39 years) much larger than non-Delta. Social distancing (SD) level 2 and SD4 in Korea were associated with transmission reduction factors of 0.64 to 0.69 and 0.70 to 0.78, respectively. The easing of NPIs to a level comparable to SD2 should be initiated not earlier than 16 October to keep the number of severe cases below the capacity of Korea's healthcare system. Simulation results also showed that a surge prompted by the spread of the Delta variant can be prevented if the number of people vaccinated daily was larger.

Simulations showed that the timing of easing and intensity of NPIs, vaccination speed, and screening measures are key factors in preventing another epidemic wave.

## 47 **1 Keywords**

48 COVID-19, Delta variant, mathematical model, maximum likelihood estima-  
49 tion, age-structure, vaccination, non-pharmaceutical interventions, Korea, so-  
50 cial distancing

## 51 **2 Key Messages**

- 52 • Maximum likelihood estimation can be utilized to determine the trans-  
53 mission rates of the Delta and non-Delta variants.
- 54 • The phase-dependent NPIs implemented by the Korean government were  
55 effectively quantified in the modelling study.
- 56 • Even with fast vaccination, resurgence of cases is still possible if NPIs are  
57 eased too early or screening measures are relaxed.
- 58 • The model can be used as a guide for policy makers on deciding appro-  
59 priate SD level that considers not only disease control, but also the socio-  
60 economic impact of maintaining strict measures.

### 61 3 Introduction

62 The coronavirus disease 2019 (COVID-19) is an ongoing pandemic caused by  
63 the severe acute respiratory syndrome coronavirus 2 (SARS-CoV-2). The rise  
64 in the number of COVID-19 cases observed worldwide since July 2021 can be  
65 attributed to the emergence of the Delta variant of SARS-CoV-2 [1]. The Delta  
66 variant significantly reduced the effectiveness of vaccines to symptomatic in-  
67 fection to about 50-70% compared to the Alpha variant [2, 3]. Nevertheless,  
68 these vaccines are reported to still be effective against severe disease, hospital-  
69 ization, and death [2, 4].

70 To mitigate the spread of COVID-19, on top of vaccination, various non-  
71 pharmaceutical interventions (NPIs), such as social distancing (SD), are still  
72 implemented concurrently. In Korea, a four-level SD plan has been imple-  
73 mented since July 2021. The plan outlines the number of persons allowed in a  
74 gathering and operational guidelines of shops, restaurants, gyms, pubs, con-  
75 cert halls, sports stadium, and other commercial facilities. Since 12 July 2021,  
76 SD level has been raised to the highest (SD4) to combat the fourth wave of  
77 COVID-19 in the Republic of Korea. As of 29 October 2021, there are 360 536  
78 confirmed cases and 2817 deaths of COVID-19 in Korea [5].

79 Vaccination in Korea began on 26 February 2021 and priority was given to  
80 the healthcare workers and elderly. The vaccination plan proceeded according  
81 to age, starting with older age group [5]. Several types of vaccines have been  
82 administered, mostly BNT162b2 or ChAdOx1 [5]. Meanwhile, the first case of  
83 a local community transmission in Korea with the Delta variant was reported  
84 on 27 April 2021. The number of cases has steeply increased since then and the  
85 proportion of the Delta variant is almost 100% among the genome-sequenced  
86 COVID-19 cases in Korea [6].

87 Transmission rates between age groups before and during the period when

88 Delta became the dominant variant of SARS-CoV-2 infections are estimated  
89 using MLE, which is a preferred parameter estimation and inference tool in  
90 statistics [7, 8]. The key factors leading the epidemic of COVID-19 recently  
91 are vaccination, variants of the virus, and implementation of SD. In this study,  
92 we developed an age-structured compartment model that captures COVID-19  
93 transmission with the Delta and non-Delta variants among vaccinated and un-  
94 vaccinated people. Furthermore, we quantify NPIs according to government  
95 policy and present scenarios that investigate the impact of timely vaccination,  
96 effective NPIs, and early detection of cases.

## 97 **4 Materials and Methods**

### 98 **4.1 Data**

99 We analyzed the COVID-19 case data including age, date of diagnosis by PCR  
100 test, and date of symptom onset from 26 February to 10 September 2021 pro-  
101 vided by the Korea Disease Control and Prevention Agency (KDCA). The data  
102 on the number of people vaccinated per day, type of vaccine, and age of the  
103 person who were vaccinated from 26 February to 8 October 2021 are available  
104 in [9].

### 105 **4.2 Mathematical model**

106 The model we develop is an extension of the models in [7, 8] to include age-  
107 specific transmission rates of the Delta and non-Delta variants. The dynamics  
108 of infection with the Delta or non-Delta variants follows an SEIQR scheme,  
109 where the subscripts  $i$  and  $v$  refer to age group and vaccination, respectively,  
110 and the superscripts  $non\delta$  or  $\delta$  refer to whether the infection is with the non-  
111 Delta or Delta variant, respectively. Eight age groups are considered: 0 to 17  
112 are referred to as group 1, 18 to 29 as group 2, and those aged 30 to 39, 40 to 49,  
113 and so on until 80 and above, are groups 3 to 8. The model diagram depicted in  
114 Figure 1 shows that susceptible ( $S$ ) and vaccinated individuals may be exposed  
115 to non-Delta or Delta variants ( $E$ ), with a force of infection  $\lambda$ , and become in-  
116 fectious ( $I$ ). Once confirmed, these individuals are isolated and categorized as  
117 mild ( $Q^m$ ) or severe ( $Q^s$ ), and eventually recover ( $R$ ) or die. Compartments  
118 for individuals who are vaccinated effectively ( $V$ ), ineffectively ( $U$ ), and then  
119 developed partial ( $P^{part}$ ) or full immunity ( $P^{full}$ ) are also considered.

120 The age-specific, vaccine-dependent parameters  $e^{part}$ ,  $e^{full}$ , and  $\omega$  consider  
121 the proportion of an age group vaccinated with either ChAdOx1 or BNT162b2

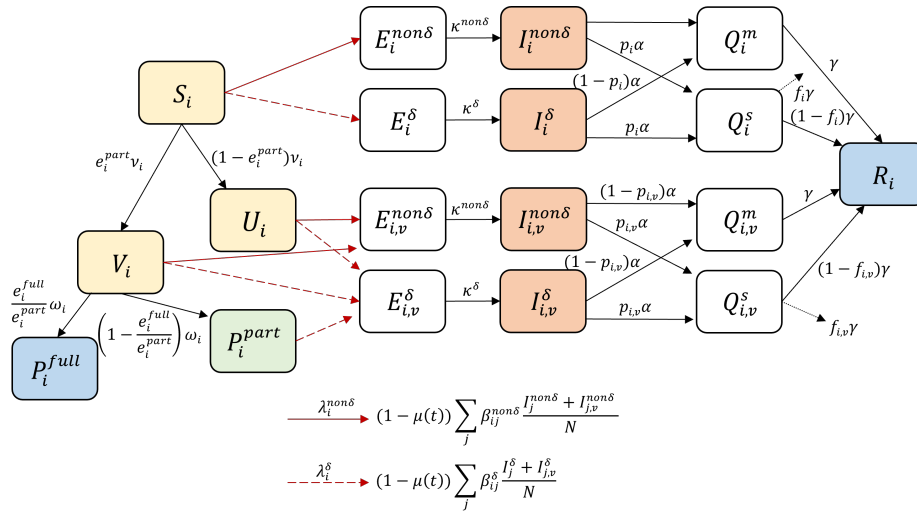


Figure 1: The model flowchart describing the transmission of COVID-19 with the non-Delta or Delta variants. The susceptible class of age group  $i$ , denoted by  $S_i$ , can be exposed to the non-Delta or Delta variants ( $E_i^{non\delta}, E_i^\delta$ ) with forces of infection  $\lambda_i^{non\delta}$  or  $\lambda_i^\delta$ , respectively. The transmission reduction factor  $\mu(t)$  quantifies the NPIs according to government policy. Also,  $S_i$  can become effectively  $V_i$  or ineffectively  $U_i$  vaccinated, depending on the daily number of vaccinated individuals  $v_i$ , and vaccine effectiveness to the non-Delta variant  $e_i^{part}$ . Individuals in  $V_i$  become partially  $P_i^{part}$  or fully protected  $P_i^{full}$  from infection after  $1/\omega_i$  days on average, or may be exposed to the non-Delta or Delta variant ( $E_{i,v}^{non\delta}, E_{i,v}^\delta$ ). Vaccine effectiveness to the Delta variant is denoted by  $e_i^{full}$ . The mean latent period of the non-Delta and Delta variants are  $1/\kappa^{non\delta}$  and  $1/\kappa^\delta$  days, respectively. The mean infectious period is  $1/\alpha$  days. Those in the infectious classes ( $I_i^{non\delta}, I_i^\delta, I_{i,v}^{non\delta}$  and  $I_{i,v}^\delta$ ) are isolated as soon as confirmed, and are classified as mild ( $Q_i^m, Q_{i,v}^m$ ) or severe ( $Q_i^s, Q_{i,v}^s$ ). Individuals in the isolated compartments may die or recover ( $R_i$ ) after  $1/\gamma$  days on average. The parameters  $p_i, p_{i,v}$  represent the proportion that becomes severe and  $f_i, f_{i,v}$  are the mean fatality rates of the unvaccinated and vaccinated individuals, respectively.

122 [10], effectiveness of these vaccines to the Delta and non-Delta variants [3],  
 123 and interval between doses [11]. The transmission rates  $\beta$  for the Delta and  
 124 non-Delta variants are estimated using MLE. The transmission reduction factor  
 125  $\mu(t)$ , which quantifies the NPIs according to government policy, is also es-  
 126 timated. The values of  $v$ ,  $p$  and  $f$  are derived from data. Details of the model

127 development are found in Appendix A.

128 We apply MLE to estimate the transmission rates of the Delta and non-Delta  
129 variants between age groups by considering two periods. Transmission rates  
130 of the non-Delta variant were estimated from the period 26 February to 30 June  
131 2021, while the data from 1 August to 10 September, when the proportion of  
132 cases with the Delta variant was over 80%, were used to estimate the transmis-  
133 sion rates for the Delta variant [12].

### 134 4.3 Modelling scenarios

135 To examine the impact of vaccination rollout, we extended the model simula-  
136 tion until 30 December 2021 and analyzed the effect of easing NPIs at different  
137 times. Considering that approximately 77% of the population already have  
138 at least one dose, we assumed that 85% of the population is vaccinated by 30  
139 November 2021. We consider three dates for the initiation of eased NPIs: 8  
140 October, 18 October, and 1 November. For each date, we simulate three scenar-  
141 ios with different values of the transmission reduction factor  $\mu(t)$ :  $\mu = 0.69$  in  
142 scenario 1 (S1),  $\mu = 0.64$  in scenario 2 (S2), and  $\mu = 0.52$  in scenario 3 (S3). The  
143 estimated value obtained from 16 April to 3 June 2021 is S1, and the minimum  
144 value estimated in this study is S2 (from 16 June to 11 July 2021). The value of  
145  $\mu$  in S3 was estimated from the third epidemic wave in 2020, when it was SD1,  
146 and is a relatively lower value compared to S2 [13].

147 We also proceeded with simulation-based experiment to study the effects  
148 of varying the speed of vaccination, arrival timing of the Delta variant, and in-  
149 tensity of NPIs. In this case, the initial condition of simulations is identical to  
150 26 February 2021 in Korea and the simulation time is set to 365 days. The total  
151 number of vaccinated people is assumed to be 40 million, which is approxi-  
152 mately 78% of the population in Korea, and the number of people vaccinated



153 daily is set to 150 000, 200 000, or 400 000. Moreover, we fix the order of vac-  
154 cination from oldest to youngest, that is, 8-7-6-5-4-3-2, excluding group 1. We  
155 denote by  $t_\delta$  the day when the individuals exposed to the Delta variant arrived  
156 in the local community, and we set its range from zero to 80 days. Note that  
157 in Korea, the date of arrival of the Delta variant corresponds to  $t_\delta = 52$ . We  
158 consider values of  $\mu$  from 0.52 to 0.78 in 0.001 increments. In total, there are 21  
159 141 simulations for the different values of  $v_i$ ,  $t_\delta$ , and  $\mu$ .

## 160 5 Results

### 161 5.1 Parameter Estimation

162 The estimated transmission rates obtained using MLE form a matrix according  
163 to the age groups. The transmission rate matrices, visualized in Figure 2, rep-  
164 resent the transmission patterns of the non-Delta (a) and Delta variants (b) in  
165 Korea.

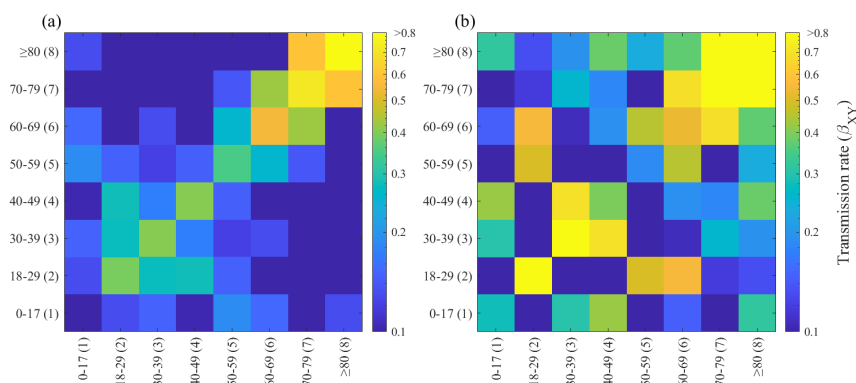


Figure 2: Estimated transmission rates among age groups (a) non-Delta variants from 26 February to 30 June 2021 and (b) Delta variant from 1 August to 10 September 2021.

166 Since the various government policies including SD implemented during  
167 the periods considered in estimating the transmission rates, we normalize the  
168 transmission rate matrices to exclude phase-dependent factors. The details of  
169 the computation are found in Appendix C.

170 We use the normalized transmission rate matrices in estimating the factor  
171  $\mu(t)$ , which represents the reduction in transmission induced by NPIs accord-  
172 ing to government policy. Table 1 presents the estimates for each phase from  
173 26 February to 8 October 2021. Figure 3 (a) shows the plots of the estimates  
174 for the reduction factor  $\mu(t)$  (red curve) with the effective reproductive num-

ber ( $\mathcal{R}_t$ , blue curve) described in Appendix C. At the start of the simulation  
 period, Seoul Capital Area was at SD2. When  $\mu(t)$  increased from 0.64 to 0.69  
 around 16 April 2021,  $\mathcal{R}_t$  decreased to 0.97 and stayed below 1 until around 16  
 June. From 16 June to 11 July,  $\mu$  was estimated at 0.64 and  $\mathcal{R}_t$  jumped to as high  
 as 1.52. The exponential rise in the proportion of cases infected with the Delta  
 variant (black solid curve in Figure 3 (a)) and daily confirmed cases (Figure 3  
 (b)) was also observed on the same period, which prompted the start of the  
 fourth wave. On 12 July, the Korean government raised the SD level in Seoul  
 Capital Area to SD4. A steep increase in the cumulative confirmed cases was  
 seen beginning 12 July (Figure 3 (c)), and the estimates for  $\mu$  were the highest  
 from this period until 06 September. At the same time, the proportion of hosts  
 having full immunity (black dashed curve in Figure 3 (a)) increased steadily,  
 reaching up to about 50% by the end of the estimation period. On the last  
 phase, the estimated value of  $\mu$  was 0.70.

Phase	Period	Value	SD Level	$\mathcal{R}_t$
1	26 Feb to 25 Mar	0.64	2	[1.13, 1.14]
2	26 Mar to 15 Apr	0.65	2	[1.11, 1.12]
3	16 Apr to 3 Jun	0.69	2	[0.96, 0.97]
4	4 Jun to 15 Jun	0.70	2	[0.94, 0.96]
5	16 Jun to 11 Jul	0.64	2	[1.16, 1.52]
6	12 Jul to 25 Jul	0.76	4	[1.03, 1.09]
7	26 Jul to 8 Aug	0.77	4	[1.07, 1.07]
8	9 Aug to 5 Sep	0.78	4	[0.91, 1.00]
9	6 Sep to 19 Sep	0.71	4	[1.11, 1.21]
10	20 Sep to 8 Oct	0.70	4	[0.94, 1.10]

Table 1: Estimates for the phase-dependent, transmission reduction factor  $\mu(t)$ , social distancing (SD) level, and range of effective reproductive number  $\mathcal{R}_t$  from 26 February to 8 October 2021.

To illustrate how  $\mu$  can be used to suggest appropriate SD level, assume

190 that the basic reproductive number of the disease is five, Delta and non-Delta  
191 variants can infect the population, 80% of population is vaccinated, and vac-  
192 cine effectiveness is 62.5%. Then without NPIs,  $\mathcal{R}_t = 5 \times 0.8 \times 0.625 = 2.5$ . To  
193 maintain an  $\mathcal{R}_t$  below one, SD2 is appropriate since the minimum estimated  
194 value of  $\mu(t)$  on SD2 was 0.64 and this translates to  $\mathcal{R}_t = (1 - 0.64) \times 2.5 = 0.9$ .  
195 On the other hand if  $\mu = 0.52$ , which represents worst case during SD1, then  
196  $\mathcal{R}_t = (1 - 0.52) \times 2.5 = 1.2$ . In this case, SD4 may not necessary and can  
197 aggravate present economic problems.

198 In Figure 4, we present the best fit of the model to the data on daily and  
199 cumulative cases per age group. The rise in the number of cases in the period  
200 from 16 June 2021 was observed across all age groups, with age 18-29 having  
201 the most and the elderly groups having the least increase. The model shows a  
202 peak (459 cases) on 16 August and another peak (519 cases) on 28 September  
203 in age 18-29. Towards the end of the simulation period, a decreasing trend  
204 in the number of cases was observed in most age groups except age 0-17, not  
205 vaccinated.

## 206 **5.2 Analysis on the timing of easing the NPIs**

207 Nine scenarios considering different dates of initiation and levels of eased NPIs  
208 are displayed in Figure 5. The red, black, and blue curves, correspond to start-  
209 ing the eased NPIs on 8 October, 18 October, and 1 November 2021, respec-  
210 tively. The solid curves represent S1, dashed curves S2, and dotted curves S3.  
211 Panel (a) shows  $\mathcal{R}_t$ , (b) the daily confirmed cases, (c) the number of severe  
212 patients requiring hospital beds, and (d) the cumulative death. The dashed  
213 grey curve in panel (c) marks the maximum number of hospital beds (1067) for  
214 severe patients in Korea [14]. Results show that the worst case scenario is S3  
215 with 8 October as easing time, wherein the peak number of daily cases, severe

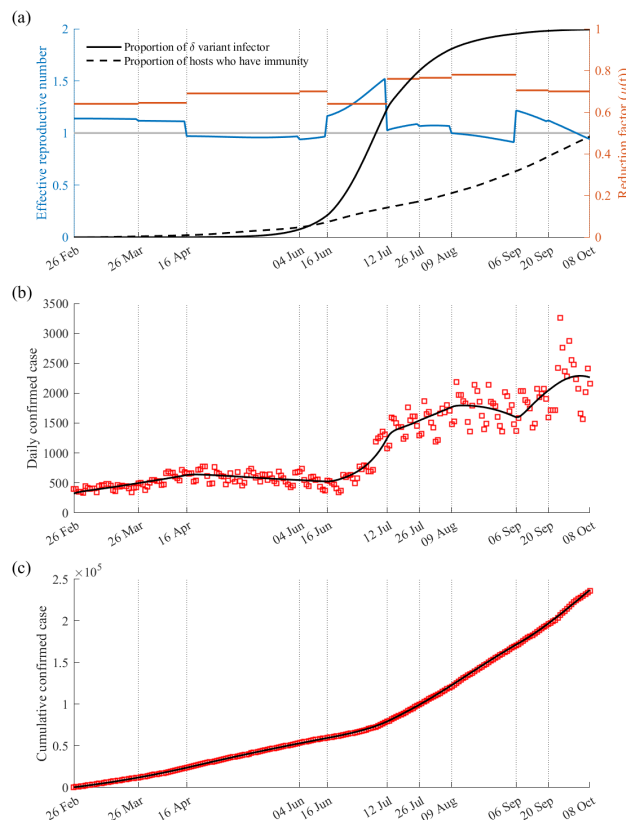


Figure 3: The parameter estimation results obtained by fitting the model to the cumulative confirmed cases. Panel (a) shows the effective reproductive number (blue), estimates of the transmission reduction factor  $\mu(t)$  (red), proportion of the active cases infected with the Delta variant (black solid curve), and proportion of the total population who has immunity (black dashed curve). Panel (b) shows the best fit of the model to the daily confirmed cases and (c) the best fit of the model to the cumulative confirmed cases. The boxes represent the data for the daily and cumulative cases from 26 February to 8 October 2021.

216 patients, and cumulative deaths could reach 8207, 1617, and 6528, respectively.  
 217 But if the easing to S3 was started later, on 18 October or 1 November, the peak  
 218 numbers could be reduced to 4385 (40.48% reduction) or 1961 (76.11% reduc-  
 219 tion) for the peak daily cases, 879 (45.64% reduction) or no increase for the peak

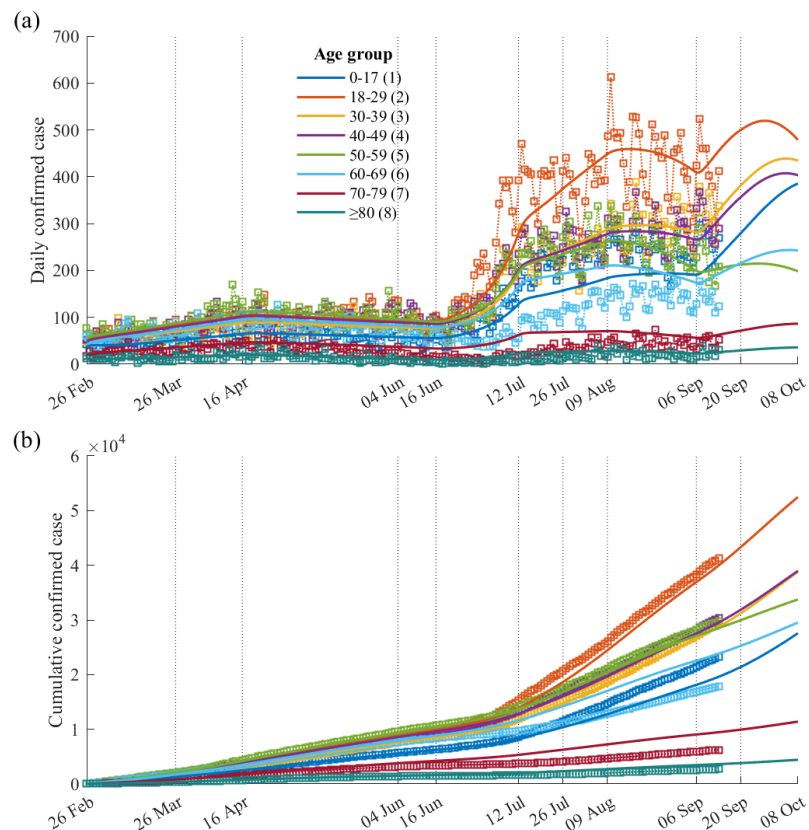


Figure 4: The best fit of the model to the (a) daily confirmed cases and (b) cumulative confirmed cases per age group. The boxes represent the data per age group from 26 February to 10 September 2021.

220 number of severe patients, and 3847 (42.07% reduction) or 2313 (64.57% reduc-  
221 tion) for the cumulative deaths, compared to when the easing was initiated  
222 earlier. The rest of the simulations show a decreasing trend of daily confirmed  
223 cases and number of severe patients. The simulations illustrate the importance  
224 of the timing of easing NPIs in preventing the occurrence of another epidemic  
225 wave. All scenarios, except the worst case, show that the number of severe  
226 patients did not reach the limit (1067) of Korea.

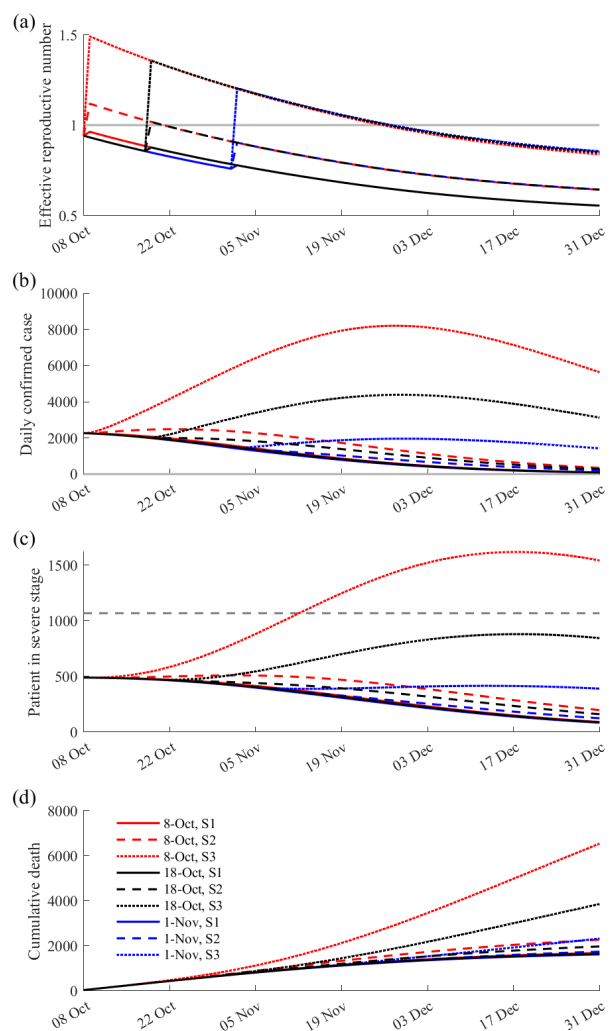


Figure 5: Results on the effect of easing NPIs at different times. Panel (a) shows the effective reproductive number, (b) number of daily confirmed cases, (c) number of severe patients requiring hospital beds, and (d) cumulative number of deaths. Colours and shapes of curves indicate the timing of initiation (8 October, 18 October, and 1 November) and level of eased NPIs (S1, S2, and S3). Grey dashed line in (c) indicates the number of available beds (1067) for severe patients in Korea.

### 227 **5.3 Analysis on the vaccination speed, NPIs, and arrival tim-** 228 **ing of the Delta variant**

229 Figure 6 displays the simulation results when  $\mu = 0.67$ ,  $t_\delta = 52$ , and  $v_i =$   
230 200 000 or 400 000. In panel (a),  $\mathcal{R}_t$  and the proportion of cases infected with  
231 the Delta variant are displayed. The magenta asterisk indicates  $t_\delta = 52$ . When  
232  $v_i = 200\,000$ ,  $\mathcal{R}_t$  increased up to 1.4, while if  $v_i = 400\,000$ ,  $\mathcal{R}_t$  decreased to  
233 below one. In panels (b) and (c), a second peak with more than 2000 cases  
234 and 600 severe patients is observed when  $v_i = 200\,000$  (red curve), whereas no  
235 second peak is observed when  $v_i = 400\,000$  (blue curve). Panel (d) shows that  
236 the cumulative deaths when  $v_i = 200\,000$  can reach 4.48 times higher compared  
237 to when  $v_i = 400\,000$ . Panels (e) and (f) display the cumulative number of cases  
238 and deaths of each age group, with 34% of the cases occurring in age group 2  
239 and 68% of the deaths occurring in age group 8 when  $v_i = 200\,000$ . These  
240 results highlight the effect of the daily number of vaccination to the occurrence  
241 of another epidemic wave.

242 Figure 7 shows a heat map summarizing the results of the 21 141 simu-  
243 lations. The columns represent the daily vaccination number ( $v_i = 150\,000$ ,  
244 200 000, and 400 000) and the rows correspond to the number of confirmed  
245 cases, deaths, and peak number of severe patients requiring hospital beds. In  
246 each panel, the  $x$  axis represents  $t_\delta$  and the  $y$  axis corresponds to  $\mu$ . The dotted  
247 red curve in panels (g), (h), and (i) marks the maximum number of hospital  
248 beds (1067) for severe patients in Korea.



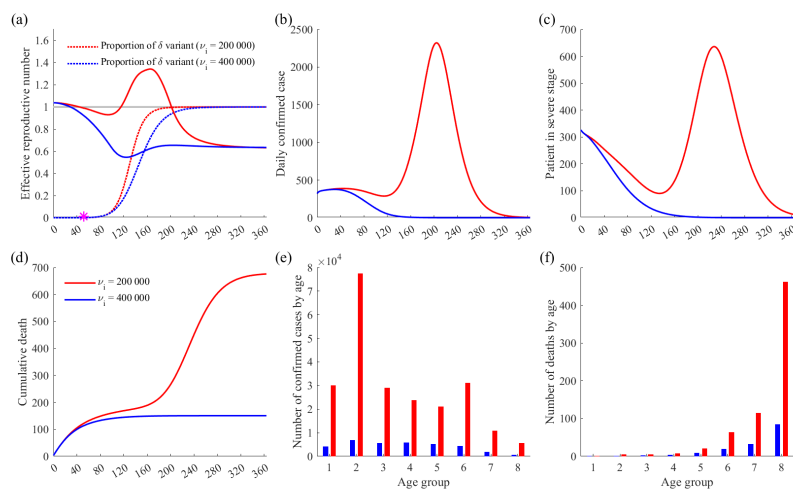


Figure 6: The simulation result with  $\mu = 0.67$ ,  $t_\delta = 52$ , and daily number of vaccination set to 200 000 or 400 000. Panel (a) shows the effective reproductive number, (b) number of daily confirmed cases, (c) number of severe patients requiring hospital beds, (d) cumulative number of deaths, (e) age-dependent number of confirmed cases, and (f) age-dependent number of deaths. Red and blue colours indicate that the number of daily administered vaccines is 200 000 and 400 000, respectively.

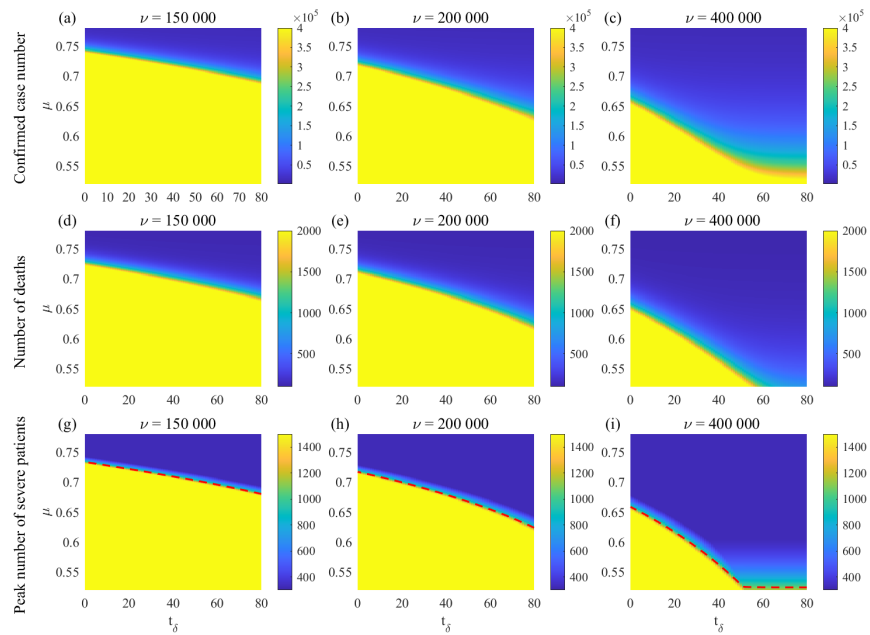


Figure 7: The simulation results of the 21,141 runs. The columns from left to right indicate the number of daily administered vaccines as 150 000, 200 000, and 400 000, respectively. Panels (a), (b), and (c) show the number of confirmed cases; (d),(e), and (f) the number of deaths; and (g),(h), and (i) the peak number of severe patients requiring hospital beds. Note that red dotted curve in panels (g),(h), and (i) indicates the maximum number of available beds (1067) for severe patients in Korea.

## 249 6 Discussion

250 The transmission rate matrix in this study was apparently different between  
251 the Delta and non-Delta variants and by age groups. The transmission rate  
252 with non-Delta variant was high between the same age groups. However,  
253 transmission with the Delta variant was much higher among age groups of  
254 18-29 and 30-39, and an increased transmission was observed between those  
255 age groups and age groups of 50-59 and 60-69. This matrix reflects the distinct  
256 epidemiologic characteristic of the COVID-19 epidemic after Delta became the  
257 dominant variant of SARS-CoV-2 in Korea: 1) incidence in younger age groups,  
258 those in 20s and 30s, increased; 2) and the major source of transmission moved  
259 from group-related or institutional outbreaks to individual contacts [15, 16].  
260 These results indicate an increased transmission with Delta variant among  
261 household contacts, which is coherent with previous studies [17, 18].

262 Higher transmission rates with the Delta variant compared to the non-Delta  
263 variant were also observed in the elderly groups, which may have resulted  
264 from breakthrough infections in nursing homes and assisted living facilities  
265 [27]. With the absence of vaccination, a much higher transmission rate with the  
266 Delta variant was expected, but was not observed in the youngest age group  
267 of 17 years old and below. This phenomenon was probably a consequence of  
268 the Korean government policy on limiting the number of attendance in school  
269 to two-thirds since October 2020 [19]. According to the data, among all the  
270 COVID-19 cases of those aged 17 years old and below in Korea, only about  
271 15% are infected from schools during this period [20].

272 We also analyzed the reduction in transmission induced by NPIs according  
273 to the government policy, presented by  $\mu(t)$ . SD2 and SD4 in Korea corre-  
274 sponded to  $\mu(t)$  values from 0.64 to 0.69, and from 0.70 to 0.78, respectively.  
275 Values of  $\mu(t)$  close to 0.7 may represent SD3 in Korea. Considering the ba-

276 sic reproductive number of a disease, vaccine effectiveness, and the amount of  
277 administered vaccines, the fitted values of  $\mu(t)$  can be an effective measures of  
278 the government policy. This parameter would be informative to the healthcare  
279 professionals and policy makers on designing prevention and control measures  
280 for emerging or reemerging infectious diseases.

281 Considering both the medical and economic impact of NPIs, the Korean  
282 government plans to reduce SD, termed 'Back to normal or With-Corona', on  
283 1 November 2021 [14]. Because vaccination and immunization takes time, we  
284 explored the effect of delaying the initiation of eased SD in Figure 5. When  
285 SD was eased to a minimal value (S3), no large-scale re-emergence of infec-  
286 tions was observed when S3 was delayed to 1 November, as opposed to when  
287 it was initiated on 8 or 18 October. In other words, gradually easing NPIs  
288 might be necessary when implementation is earlier. For example, in Korea, the  
289 maximum number of people allowed in a private gathering after 6:00PM be-  
290 came four (ten for fully vaccinated) from two since 18 October, although SD  
291 remained at SD4 [21].

292 In our generalized simulation on the effects of vaccination and NPIs, the  
293 larger reduction of transmission factor ( $\mu(t)$ ) and faster vaccination rollout  
294 or earlier implementation of stricter NPIs (e.g., expanding genomic testing to  
295 people entering from high-risk countries or elevating SD) resulted in less inci-  
296 dence, severe cases, and deaths. We are aware that the supply of vaccines is not  
297 enough globally, but fast administration of vaccines can block the occurrence  
298 of another wave. In other words, epidemic can be controllable and stable if the  
299 vaccination speed is faster.

300 There are several limitations of this research. First, the contact pattern in the  
301 matrices was already affected by NPIs and might be not identical to the contact  
302 pattern before COVID-19, necessitating the normalization done on the matri-

303 ces. For example, transmission rate among those age 0-17 might be underes-  
304 timated because of restricted attendance in schools. Second, vaccine waning  
305 is not considered. However, booster shots are administered and vaccine hes-  
306 itancy remains low in Korea, which mean that the effect of administered vac-  
307 cines might be maintained [22]. Third, our age-age matrix focused on the Delta  
308 variant, and we were not able to examine transmission of other previous vari-  
309 ants. The coverage of genomic surveillance among COVID-19 cases in Korea  
310 has steadily increased, and it covers about 30% of all confirmed cases. There-  
311 fore, the number of cases with genomic results before the occurrence of the  
312 Delta variant was small to be analyzed separately by variant types. Our result  
313 highlighted the transmission pattern of Delta, which is currently the dominant  
314 variant in most countries.

## 315 **7 Conclusion**

316 This study illustrated the higher transmissibility of the Delta relative to the  
317 non-Delta variant among various age groups in Korea by developing the trans-  
318 mission rate matrix based on MLE. The method used to quantify the effects of  
319 the vaccination and NPIs simultaneously. The model simulation results em-  
320 phasize the importance of simultaneously applying interventions, such as SD,  
321 screening measures at the entry points, and vaccination. Another epidemic  
322 wave can be avoided if a strict SD policy is not relaxed too early. Transmis-  
323 sion rate of the Delta variant of COVID-19 is high and oral treatment has not  
324 yet been provided widely, but the epidemic is still ongoing, so we suggest that  
325 NPIs are still necessary to control the epidemic and reduce the number of se-  
326 vere cases to prevent a burden to the healthcare system. Even with the same  
327 SD level, model simulations showed that outcomes may change depending on  
328 vaccine administration and emergence of a highly transmissible variant. If vac-  
329 cination is slow, then NPIs should be strictly implemented to lessen the medical  
330 and socio-economic burden of COVID-19 to the society.

## 331 **8 Ethics approval**

332 The study was conducted according to the guidelines of the Declaration of  
333 Helsinki, and approved by the Institutional Review Board of Konkuk Univer-  
334 sity (7001355-202101-E-130)

## 335 **9 Funding**

336 This paper is supported by the Korea National Research Foundation (NRF)  
337 grant funded by the Korean government (MEST) (NRF-2021M3E5E308120711).

338 This paper is also supported by the Korea National Research Foundation (NRF)  
339 grant funded by the Korean government (MEST) (NRF-2021R1A2C100448711).

## 340 **Appendix A Development of the mathematical model**

341 Susceptible individuals in age group  $i$ , denoted by  $S_i$  ( $i = 1, 2, \dots, 8$ ), who are  
342 unvaccinated become exposed to the non-Delta  $E_i^{non\delta}$  or Delta  $E_i^\delta$  variants with  
343 forces of infection  $\lambda_i^{non\delta}$  or  $\lambda_i^\delta$ , respectively. These exposed individuals become  
344 infectious  $I_i^{non\delta}$  after  $1/\kappa^{non\delta}$  or  $I_i^\delta$  after  $1/\kappa^\delta$  days. Here we assume that the  
345 latent period of infection with the Delta variant is shorter than the non-Delta  
346 variant [23, 24].

347 To account for vaccination, individuals in  $S_i$  can become effectively  $V_i$  or  
348 ineffectively  $U_i$  vaccinated, depending on the daily number of vaccinated in-  
349 dividuals in age group  $i$ , denoted by  $\nu_i$ , and vaccine effectiveness to the non-  
350 Delta variant  $e_i^{part}$ . Individuals in  $V_i$  eventually become partially  $P_i^{part}$  or fully  
351 protected/immune  $P_i^{full}$  from infection after  $1/\omega_i$  days. Fully protected in-  
352 dividuals are assumed to be immune to COVID-19, while partially protected  
353 individuals can only be infected with the Delta variant. Vaccinated individ-  
354 uals who are exposed to the non-Delta  $E_{i,v}^{non\delta}$  or Delta  $E_{i,v}^\delta$  variant eventually  
355 progress to the vaccinated infectious classes  $I_{i,v}^{non\delta}$  or  $I_{i,v}^\delta$ .

356 We assume that individuals in the infectious classes ( $I_i^{non\delta}$ ,  $I_i^\delta$ ,  $I_{i,v}^{non\delta}$  and  $I_{i,v}^\delta$ )  
357 are isolated as soon as they were confirmed, and are classified as mild ( $Q_i^m$ ,  
358  $Q_{i,v}^m$ ) or severe ( $Q_i^s$ ,  $Q_{i,v}^s$ ). The mean infectious period of an infected individual  
359 is  $1/\alpha$  days, and  $p_i$  or  $p_{i,v}$  denote the proportions that an infected unvaccinated  
360 or vaccinated individual progresses to a severe case. Individuals in the isolated  
361 compartments recover  $1/\gamma$  days on average and the mean fatality rates of the  
362 unvaccinated and vaccinated groups are denoted by  $f_i$  and  $f_{i,v}$ , respectively.

The following system of ordinary differential equations describes the de-

veloped age-structured model:

$$\begin{aligned}
 \frac{dS_i}{dt} &= -(\lambda_i^{non\delta} + \lambda_i^\delta)S_i - v_i, \\
 \begin{cases} \frac{dE_i^{non\delta}}{dt} = \lambda_i^{non\delta}S_i - \kappa^{non\delta}E_i^{non\delta}, & \frac{dE_i^\delta}{dt} = \lambda_i^\delta S_i - \kappa^\delta E_i^\delta, \\ \frac{dE_{i,v}^{non\delta}}{dt} = \lambda_i^{non\delta}(U_i + V_i) - \kappa^{non\delta}E_{i,v}^{non\delta}, & \frac{dE_{i,v}^\delta}{dt} = \lambda_i^\delta(U_i + V_i + P_i^{part}) - \kappa^\delta E_{i,v}^\delta, \end{cases} \\
 \begin{cases} \frac{dI_i^{non\delta}}{dt} = \kappa^\delta E_i^{non\delta} - \alpha I_i^{non\delta}, & \frac{dI_i^\delta}{dt} = \kappa^{non\delta}E_i^\delta - \alpha I_i^\delta, \\ \frac{dI_{i,v}^{non\delta}}{dt} = \kappa^{non\delta}E_{i,v}^{non\delta} - \alpha I_{i,v}^{non\delta}, & \frac{dI_{i,v}^\delta}{dt} = \kappa^\delta E_{i,v}^\delta - \alpha I_{i,v}^\delta, \end{cases} \\
 \begin{cases} \frac{dQ_i^m}{dt} = \alpha(1 - p_i)(I_i^{non\delta} + I_i^\delta) - \gamma Q_i^m, & \frac{dQ_i^s}{dt} = \alpha p_i(I_i^{non\delta} + I_i^\delta) - \gamma Q_i^s, \\ \frac{dQ_{i,v}^m}{dt} = \alpha(1 - p_{i,v})(I_{i,v}^{non\delta} + I_{i,v}^\delta) - \gamma Q_{i,v}^m, & \frac{dQ_{i,v}^s}{dt} = \alpha p_{i,v}(I_{i,v}^{non\delta} + I_{i,v}^\delta) - \gamma Q_{i,v}^s, \end{cases} \\
 \frac{dR_i}{dt} &= \gamma(Q_i^m + (1 - f_i)Q_i^s + Q_{i,v}^m + (1 - f_{i,v})Q_{i,v}^s), \\
 \frac{dU_i}{dt} &= (1 - e_i^{part})v_i - (\lambda_i^{non\delta} + \lambda_i^\delta)U_i, \\
 \frac{dV_i}{dt} &= e_i^{part}v_i - (\lambda_i^{non\delta} + \lambda_i^\delta)V_i - \omega_i V_i, \\
 \frac{dP_i^{part}}{dt} &= \left(1 - \frac{e_i^{full}}{e_i^{part}}\right)\omega_i V_i - \lambda_i^\delta P_i^{part}, \\
 \frac{dP_i^{full}}{dt} &= \frac{e_i^{full}}{e_i^{part}}\omega_i V_i,
 \end{aligned}$$

where the forces of infection  $\lambda_i^{non\delta}$  and  $\lambda_i^\delta$  are defined as

$$\begin{aligned}
 \lambda_i^{non\delta}(t) &= (1 - \mu(t)) \sum_{j=1}^8 \beta_{ij}^{non\delta} \frac{I_j^{non\delta} + I_{j,v}^{non\delta}}{N}, \\
 \lambda_i^\delta(t) &= (1 - \mu(t)) \sum_{j=1}^8 \beta_{ij}^\delta \frac{I_j^\delta + I_{j,v}^\delta}{N},
 \end{aligned}$$

$\mu(t)$  is the phase-dependent, transmission reduction factor accounting for NPIs and its estimated values are in Table 1,  $\beta_{ij}^{non\delta}$  and  $\beta_{ij}^\delta$  are the transmission rates



between age groups, and

$$N = \sum_{i=1}^8 \left( S_i + E_i^{non\delta} + E_i^{\delta} + E_{i,v}^{non\delta} + E_{i,v}^{\delta} + I_i^{non\delta} + I_i^{\delta} + I_{i,v}^{non\delta} + I_{i,v}^{\delta} + R_i + U_i + V_i + P_i^{part} + P_i^{full} \right).$$

363 Tables 2 and 3 summarize the age-specific and non-age-specific model param-  
 364 eters and their values.

Symbol	Description	Value	Reference
$1/\kappa^{non\delta}$	Mean latent period of the non-Delta variant	4 days	[23, 24]
$1/\kappa^{\delta}$	Mean latent period of the Delta variant	2 days	[23, 24]
$1/\alpha$	Mean infectious period	6 days	[24, 25]
$1/\gamma$	Mean duration of isolation (hospitalization)	20 days	[26]

Table 2: Non-age-specific parameters of the model.

365 Table 4 shows the vaccine effectiveness of ChAdOx1 and BNT162b2 to the  
 366 non-Delta and Delta variants after the first and second doses. Table 5 shows  
 367 the proportion of each age group vaccinated with ChAdOx1, and the calcu-  
 368 lated values of  $e_i^{part}$ ,  $e_i^{full}$  and  $\omega_i$ . The average duration from the first dose to  
 369 having immunity ( $1/\omega_i$ ) and vaccine effectiveness to the non-Delta and Delta  
 370 variants ( $e_i^{part}$ ,  $e_i^{full}$ ) of each age group are calculated depending on the vaccine  
 371 effectiveness and type of vaccine given to a proportion of an age group. We  
 372 assume that the interval between doses of ChAdOx1 and BNT152b2 are 11 and  
 373 4 weeks, respectively.

Symbol	Description	Age group							
		1	2	3	4	5	6	7	8
$p_i$	Proportion of unvaccinated group $i$ that becomes severe	0	0	0.01	0.02	0.04	0.07	0.13	0.26
$p_{i,v}$	Proportion of vaccinated group $i$ that becomes severe	0	0	0	0.01	0.01	0.03	0.02	0.05
$f_i$	Mean fatality rate of unvaccinated group $i$ (1/day)	0	0	0	0	0	0.01	0.03	0.13
$f_{i,v}$	Mean fatality rate of vaccinated group $i$ (1/day)	0	0	0	0	0	0	0	0.01
$e_i^{part}$	Vaccine effectiveness to non-Delta	0.94	0.93	0.91	0.9	0.91	0.76	0.83	0.92
$e_i^{full}$	Vaccine effectiveness to Delta	0.88	0.87	0.85	0.84	0.85	0.69	0.76	0.86
$1/\omega_i$	Mean interval from first dose to immunity (1/day)	35.44	36.4	40.12	41.91	39.44	64.08	52.52	38.95

Table 3: Age-specific parameters of the model calculated using data from [10, 11] and vaccine effectiveness summarized in Table 4.

	ChAdOx1		BNT162b2	
	First dose	Second dose	First dose	Second dose
Vaccine effectiveness to the non-Delta variant	0.49	0.74	0.47	0.94
Vaccine effectiveness to the Delta variant	0.30	0.67	0.36	0.88

Table 4: Vaccine effectiveness of ChAdOx1 and BNT162b2 to the non-Delta and Delta variants depending on the number of doses [3].

Description	Age group							
	1	2	3	4	5	6	7	8
Proportion of age group $i$ administered with ChAdOx1	0.00	0.03	0.15	0.21	0.13	0.93	0.55	0.11
$e_i^{part}$	0.94	0.93	0.91	0.9	0.91	0.76	0.83	0.92
$e_i^{full}$	0.88	0.87	0.85	0.84	0.85	0.69	0.76	0.86
$1/\omega_i$ (days)	35.44	36.40	40.12	41.91	39.44	64.08	52.52	38.95

Table 5: Proportion of age group  $i$  administered with ChAdOx1 from data [10] and the calculated age-dependent vaccine effectiveness to the Delta and non-Delta variants, and average duration to develop full immunity.

## 374 Appendix B MLE formulation

To establish the likelihood function to be optimized, we first divide each age group into three subgroups to distinguish COVID-19 outcomes: infected ( $\Lambda_{Ii}$ ), unvaccinated and uninfected ( $\Lambda_{Si}$ ), and effectively vaccinated and uninfected ( $\Lambda_{Vi}$ ), where  $i$  indicates the age group. Let  $\beta_{XY}$  be the transmission rate from age group  $Y$  to  $X$ . Assuming a homogeneous mixing of the population, and that the transmission events are exponentially distributed, the probability that an individual  $x$  in subgroup  $\Lambda$  at the time  $t - 1$  is still uninfected until the next time  $t$  is given by

$$p_{S,\Lambda,x}(t) = \exp\left(-\frac{\sum_j \beta_{ij} \mathbf{I}_j(t-1)}{N}\right),$$

375 where  $\mathbf{I}_j(t-1)$  denotes the number of hosts in group  $j$  which can spread the  
376 disease at time  $t - 1$ , and  $N$  is the total population. We can set  $N$  as a constant  
377 because the number of isolated individuals (or deceased) is less than 0.02%  
378 of the population. On the other hand, the probability that an individual  $x$  in

379 group  $\Lambda$  is uninfected at the time  $t - 1$  but becomes infected at  $t$  is

$$p_{I,\Lambda,x}(t) = 1 - \exp\left(-\frac{\sum \beta_{ij} \mathbf{I}_j(t-1)}{N}\right).$$

380 Hence, an individual who stays uninfected until final time  $t_f$  has probabilities

381  $p_{S,\Lambda,x}(t)$  at each time until  $t_f$ . In addition, an individual can be vaccinated at

382 time  $t_{V_i,x}$ , have immunity after  $t_{e,i}$  days, and stay uninfected until final time  $t_f$ .

383 An individual infected at time  $t_{I_i,x}$  has probabilities  $p_{S,\Lambda,x}(t)$  until  $t_{I_i,x} - 1$  and

384  $p_{I_i,\Lambda,x}(t_{I_i,x})$ .

The likelihood function  $L$  is formulated as

$$L = \prod_i (L_{1,i} \cdot L_{2,i} \cdot L_{3,i}),$$

where

$$L_{1,i} = \prod_{x \in \Lambda_{Si}} \left( \prod_{t=0}^{t_f} p_{S_i,x}(t) \right),$$

$$L_{2,i} = \prod_{x \in \Lambda_{Vi}} \left( \prod_{t=0}^{\min\{t_f, t_{V_i,x} + t_{e,i}\}} p_{S,\Lambda_{Vi},x}(t) \right),$$

$$L_{3,i} = \prod_{x \in \Lambda_{Ii}} \left( \prod_{t=0}^{t_{I_i,x}-1} p_{S,\Lambda_{Ii},x}(t) \right) p_{I,\Lambda_{Ii},x}(t_{I_i,x}).$$

385 By taking the logarithm of  $L$  and using the optimization toolbox in MATLAB,

386 we obtain a matrix containing the transmission rates of the Delta and non-Delta

387 variants between age groups.

## 388 Appendix C Normalized transmission rate matrices 389 and the effective reproductive number

390 Let the transmission rate matrices estimated from 26 February to 30 June and  
391 from 01 August to 10 September be  $M_{est}^{non\delta}$  and  $M_{est}^{\delta}$ , respectively. First, the re-  
392 productive number of COVID-19 using  $M_{est}^{non\delta}$  is calculated via the next-generation-  
393 matrix method and denoted as  $\mathcal{R}_{est}^{non\delta}$ . Second, a normalized transmission rate  
394 matrix of the non-Delta variant,  $M^{non\delta}$ , is formulated as  $M^{non\delta} = M_{est}^{non\delta} \mathcal{R}_0^{non\delta} / \mathcal{R}_{est}^{non\delta}$ ,  
395 where  $\mathcal{R}_0^{non\delta}$ , equal to 3.17, is the basic reproductive number of COVID-19 esti-  
396 mated from various studies before Delta variant became the major strain [27].  
397 Third, a normalized transmission rate matrix of the Delta variant is formulated  
398 similarly as  $M^{\delta} = M_{est}^{\delta} \mathcal{R}_0^{\delta} / \mathcal{R}_{est}^{\delta}$ , where  $\mathcal{R}_0^{\delta}$  is reproductive number calculated  
399 using  $M_{est}^{\delta}$  and  $\mathcal{R}_0^{\delta} = 1.97 \mathcal{R}_0^{non\delta}$  [28]. The normalized transmission rate matri-  
400 ces,  $M^{non\delta}$  and  $M^{\delta}$ , are used in this research.

401 The effective reproductive number  $\mathcal{R}_t$  is a time-dependent measure of the  
402 average number of secondary cases from a single infectious individual [29]. In  
403 this study,  $\mathcal{R}_t$  is calculated using the next-generation matrix method [30]. Us-  
404 ing the normalized transmission rate matrices,  $\mathcal{R}_t$  of the non-Delta and Delta  
405 variants are 3.17 and 6.24, respectively, if there are no NPIs and behavior change.

## 406 References

- 407 [1] Lianlian Bian, Qiushuang Gao, Fan Gao, Qian Wang, Qian He, Xing Wu,  
408 Qunying Mao, Miao Xu, and Zhenglun Liang. Impact of the delta vari-  
409 ant on vaccine efficacy and response strategies. *Expert Review of Vaccines*,  
410 0(0):1–9, 2021. PMID: 34488546.

- 411 [2] WHO Situation Reports. [https://www.who.int/publications/m/item/](https://www.who.int/publications/m/item/weekly-epidemiological-update-on-covid-19---5-october-2021)  
412 [weekly-epidemiological-update-on-covid-19---5-october-2021](https://www.who.int/publications/m/item/weekly-epidemiological-update-on-covid-19---5-october-2021).  
413 Accessed: October 6, 2021.
- 414 [3] Jamie Lopez Bernal, Nick Andrews, Charlotte Gower, Eileen Gallagher,  
415 Ruth Simmons, Simon Thelwall, Julia Stowe, Elise Tessier, Natalie Groves,  
416 Gavin Dabrera, et al. Effectiveness of covid-19 vaccines against the b.  
417 1.617. 2 (delta) variant. *N Engl J Med*, pages 585–594, 2021.
- 418 [4] Centers for Disease Control and Prevention, National Center for  
419 Immunization and Respiratory Diseases (NCIRD), Division of Vi-  
420 ral Diseases, U.S. Science Brief: COVID-19 Vaccines and Vac-  
421 cination. [https://www.cdc.gov/coronavirus/2019-ncov/science/](https://www.cdc.gov/coronavirus/2019-ncov/science/science-briefs/fully-vaccinated-people.html)  
422 [science-briefs/fully-vaccinated-people.html](https://www.cdc.gov/coronavirus/2019-ncov/science/science-briefs/fully-vaccinated-people.html). Accessed: October 6,  
423 2021.
- 424 [5] Ministry of Health and Welfare, Republic of Korea. Coronavirus disease  
425 2019 (COVID-19). <http://ncov.mohw.go.kr/en/>. Accessed: October 6,  
426 2021.
- 427 [6] Korea Disease Control and Prevention Agency; Proportions of variants  
428 among sampled genome sequencing in Korea. [https://kdca.go.kr/](https://kdca.go.kr/contents.es?mid=a20107040000)  
429 [contents.es?mid=a20107040000](https://kdca.go.kr/contents.es?mid=a20107040000). Accessed: October 27, 2021.
- 430 [7] Youngsuk Ko, Jacob Lee, Yeonju Kim, Donghyok Kwon, and Eunok Jung.  
431 COVID-19 Vaccine Priority Strategy Using a Heterogenous Transmission  
432 Model Based on Maximum Likelihood Estimation in the Republic of Ko-  
433 rea. *International Journal of Environmental Research and Public Health*, 18(12),  
434 2021.

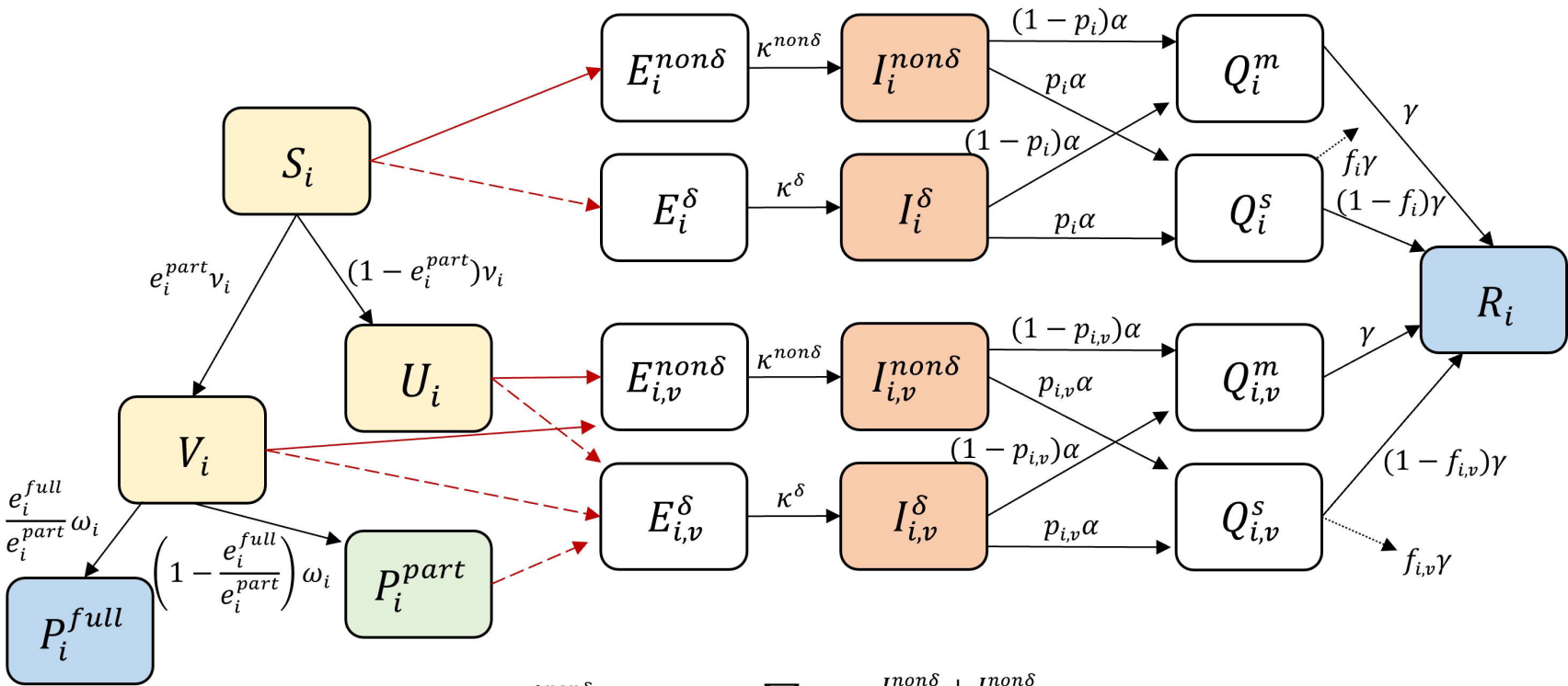
- 435 [8] Youngsuk Ko, Jacob Lee, Yubin Seo, and Eunok Jung. Risk of COVID-19  
436 transmission in heterogeneous age groups and effective vaccination strat-  
437 egy in Korea: A mathematical modeling study. *EpiH*, 2021.
- 438 [9] Korea Disease Control and Prevention Agency; Who will have vaccine  
439 first? <https://ncv.kdca.go.kr/menu.es?mid=a10117010000>. Accessed:  
440 October 14, 2021.
- 441 [10] Korea Disease Control and Prevention Agency; Korean situation report  
442 of COVID-19; 2021 October 8. [http://ncov.mohw.go.kr/tcmBoardView.  
443 do?brdId=3&brdGubun=31&dataGubun=&ncvContSeq=5989&contSeq=  
444 5989&board\\_id=312&gubun=ALL](http://ncov.mohw.go.kr/tcmBoardView.do?brdId=3&brdGubun=31&dataGubun=&ncvContSeq=5989&contSeq=5989&board_id=312&gubun=ALL). Accessed: October 14, 2021.
- 445 [11] Korea Disease Control and Prevention Agency, Questions and answers  
446 about COVID-19 vaccines, criteria for the implementation of COVID-19  
447 vaccination. <https://ncv.kdca.go.kr/menu.es?mid=a12207000000>. Ac-  
448 cessed: October 14, 2021.
- 449 [12] YTN science, Delta variant takes 96.7% among variants and  
450 number of cases for a week was 2555, 7467 in total. [https:  
451 //science.ytn.co.kr/program/program\\_view.php?s\\_mcd=0082&key=  
452 202108101604183996&page=2](https://science.ytn.co.kr/program/program_view.php?s_mcd=0082&key=202108101604183996&page=2). Accessed: October 14, 2021.
- 453 [13] National Institute for Mathematical Sciences, COVID-19 forecasts us-  
454 ing mathematical modeling. [https://www.nims.re.kr/research/post/  
455 covid19\\_2/34405](https://www.nims.re.kr/research/post/covid19_2/34405). Accessed: October 14, 2021.
- 456 [14] The Ministry of Health and Welfare, Plan of the step-by-step recovery  
457 from COVID-19. [http://www.mohw.go.kr/react/al/sal0301vw.jsp?  
458 PAR\\_MENU\\_ID=04&MENU\\_ID=0403&page=1&CONT\\_SEQ=368237](http://www.mohw.go.kr/react/al/sal0301vw.jsp?PAR_MENU_ID=04&MENU_ID=0403&page=1&CONT_SEQ=368237). Accessed:  
459 October 14, 2021.

- 460 [15] Kim Youngwha, Kim Yuyeon, Hansol Yum, Jinwha Jang, Inseop Hwang,  
461 Gwang Suk Park, Youngjun Park, Sangwon Lee, and Donghyeok Kwon.  
462 Annual covid-19 occurrence report. *Korea Disease Control and Prevention*  
463 *Agency: Weekly health and diseases*, 14(9), 2021.
- 464 [16] Korea Disease Control and Prevention Agency; Korean situation report of  
465 COVID-19; 2021 October 27. [http://ncov.mohw.go.kr/tcmBoardView.do?brdId=3&brdGubun=31&dataGubun=&ncvContSeq=6043&contSeq=6043&board\\_id=312&gubun=ALL](http://ncov.mohw.go.kr/tcmBoardView.do?brdId=3&brdGubun=31&dataGubun=&ncvContSeq=6043&contSeq=6043&board_id=312&gubun=ALL). Accessed: October 27, 2021.
- 468 [17] Kendra Dougherty, Mike Mannell, Ozair Naqvi, Dakota Matson, and Jo-  
469 lianne Stone. Sars-cov-2 b. 1.617. 2 (delta) variant covid-19 outbreak asso-  
470 ciated with a gymnastics facility—oklahoma, april–may 2021. *Morbidity*  
471 *and Mortality Weekly Report*, 70(28):1004, 2021.
- 472 [18] Elisabeth Mahase. Delta variant: What is happening with transmission,  
473 hospital admissions, and restrictions?, 2021.
- 474 [19] Ministry of Education, Announce about school operation plan after  
475 Chuseok holiday. <https://www.korea.kr/news/policyNewsView.do?newsId=148878606>. Accessed: October 14, 2021.
- 477 [20] Jinhwa Jang, Myung-Jae Hwang, Shin Young Park, Seong-Sun Kim,  
478 Jemma Park, Hansol Yeom, Su Bin Park, and Kwon Donghyoks. Trends in  
479 covid-19 cases among children and adolescents aged 0-18 years in the re-  
480 public of korea. *Korea Disease Control and Prevention Agency: Weekly health*  
481 *and diseases*, 14(42), 2021.
- 482 [21] Korea Disease Control and Prevention Agency, Anounce about  
483 the adjustment of social distancing. [http://ncov.mohw.go.kr/infoBoardView.do?brdId=3&brdGubun=32&dataGubun=&ncvContSeq=6009&contSeq=6009&board\\_id=&gubun=](http://ncov.mohw.go.kr/infoBoardView.do?brdId=3&brdGubun=32&dataGubun=&ncvContSeq=6009&contSeq=6009&board_id=&gubun=). Accessed: October 14, 2021.



- 486 [22] Hyun Kyung Park, Ji Hye Ham, Deok Hyun Jang, Jin Yong Lee, and  
487 Won Mo Jang. Political ideologies, government trust, and covid-19 vac-  
488 cine hesitancy in south korea: A cross-sectional survey. *International Jour-  
489 nal of Environmental Research and Public Health*, 18(20):10655, 2021.
- 490 [23] Yaping Wang, Ruchong Chen, Fengyu Hu, Yun Lan, Zhaowei Yang, Chen  
491 Zhan, Jingrong Shi, Xizi Deng, Mei Jiang, Shuxin Zhong, et al. Transmis-  
492 sion, viral kinetics and clinical characteristics of the emergent sars-cov-2  
493 delta voc in guangzhou, china. *EClinicalMedicine*, 40:101129, 2021.
- 494 [24] World Health Organization et al. Transmission of sars-cov-2: implications  
495 for infection prevention precautions: scientific brief, 09 july 2020. Techni-  
496 cal report, World Health Organization, 2020.
- 497 [25] Moran Ki et al. Epidemiologic characteristics of early cases with 2019  
498 novel coronavirus (2019-ncov) disease in korea. *Epidemiology and health*,  
499 42, 2020.
- 500 [26] Yong-Hoon Lee, Chae Moon Hong, Dae Hyun Kim, Taek Hoo Lee, and  
501 Jaetae Lee. Clinical course of asymptomatic and mildly symptomatic pa-  
502 tients with coronavirus disease admitted to community treatment centers,  
503 south korea. *Emerging infectious diseases*, 26(10):2346, 2020.
- 504 [27] Md Arif Billah, Md Mamun Miah, and Md Nuruzzaman Khan. Repro-  
505 ductive number of coronavirus: A systematic review and meta-analysis  
506 based on global level evidence. *PloS one*, 15(11):e0242128, 2020.
- 507 [28] Finlay Campbell, Brett Archer, Henry Laurenson-Schafer, Yuka Jinnai,  
508 Franck Konings, Neale Batra, Boris Pavlin, Katelijn Vandemaele, Maria D  
509 Van Kerkhove, Thibaut Jombart, et al. Increased transmissibility and  
510 global spread of sars-cov-2 variants of concern as at june 2021. *Eurosurveil-  
511 lance*, 26(24):2100509, 2021.

- 512 [29] Hiroshi Nishiura and Gerardo Chowell. *The Effective Reproduction Number*  
513 *as a Prelude to Statistical Estimation of Time-Dependent Epidemic Trends*, pages  
514 103–121. Springer Netherlands, Dordrecht, 2009.
- 515 [30] Odo Diekmann, JAP Heesterbeek, and Michael G Roberts. The con-  
516 struction of next-generation matrices for compartmental epidemic mod-  
517 els. *Journal of the Royal Society Interface*, 7(47):873–885, 2010.



$$\lambda_i^{non\delta} \rightarrow (1 - \mu(t)) \sum_j \beta_{ij}^{non\delta} \frac{I_j^{non\delta} + I_{j,v}^{non\delta}}{N}$$

$$\lambda_i^\delta \rightarrow (1 - \mu(t)) \sum_j \beta_{ij}^\delta \frac{I_j^\delta + I_{j,v}^\delta}{N}$$

